Downregulation of Dickkopf-3 disrupts prostate acinar morphogenesis through TGF-β/Smad signalling

Diana Romero[1],[§], Yoshiaki Kawano[1],[*],[§], Nora Bengoa[2], Marjorie M. Walker[3],[‡], Nicole Maltry[4], Christof Niehrs[4],[5], Jonathan Waxman[1] and Robert Kypta[1],[2],[¶]

[1]Department of Surgery and Cancer, Imperial College London, London, W12 0NN, UK
[2]Cell Biology and Stem Cells Unit, CIC bioGUNE, Bilbao, Spain
[3]Centre for Pathology, Imperial College London, St Mary's Hospital, London, W2 1NY, UK
[4]German Cancer Research Center, Heidelberg, 69120, Germany
[5]Institute of Molecular Biology, Mainz, 55128, Germany

*Present address: Department of Urology, Kumamoto University, Kumamoto, Japan
‡Present address: School of Medicine and Public Health, University of Newcastle, Australia
§These authors contributed equally to this work
¶Author for correspondence (r.kypta@imperial.ac.uk; rkypta@cicbiogune.es)

Summary

Loss of tissue organization is a hallmark of the early stages of cancer, and there is considerable interest in proteins that maintain normal tissue architecture. Prostate epithelial cells cultured in Matrigel form three-dimensional acini that mimic aspects of prostate gland development. The organization of these structures requires the tumor suppressor Dickkopf-3 (Dkk-3), a divergent member of the Dkk family of secreted Wnt signalling antagonists that is frequently downregulated in prostate cancer. To gain further insight into the function of Dkk-3 in the prostate, we compared the prostates of *Dkk3*-null mice with those of control littermates. We found increased proliferation of prostate epithelial cells in the mutant mice and changes in prostate tissue organization. Consistent with these observations, cell proliferation was elevated in acini formed by human prostate epithelial cells stably silenced for Dkk-3. Silencing of Dkk-3 increased TGF-β/Smad signalling, and inhibitors of TGF-β/Smad signalling rescued the defective acinar phenotype caused by loss of Dkk-3. These findings suggest that Dkk-3 maintains the structural integrity of the prostate gland by limiting TGF-β/Smad signalling.

Key words: Dkk-3, Prostate, Acinar morphogenesis, TGF-β

Introduction

Dickkopf-3 (Dkk-3) was first identified as a divergent member of the Dkk family of secreted Wnt signalling antagonists (Glinka et al., 1998; Krupnik et al., 1999; Veeck and Dahl, 2012). *DKK3* was also cloned as a gene with very low expression in a panel of human tumor-derived cell lines and named REIC (for reduced expression in immortalized cells) (Tsuji et al., 2000). In prostate cancer, Dkk-3 levels are low in poorly differentiated high Gleason score tumors (Zenzmaier et al., 2008), and ectopic expression of Dkk-3 inhibits prostate cancer cell proliferation *in vitro* and *in vivo* (Chen et al., 2009b; Edamura et al., 2007; Kawano et al., 2006). A variety of mechanisms have been proposed to account for the inhibitory effects of Dkk-3 on tumor cell proliferation in cancer of the prostate and other organs (Abarzua et al., 2005; Kashiwakura et al., 2008; Lee et al., 2009; Lodygin et al., 2005; Yue et al., 2008). Despite the tumor suppressor activities of Dkk-3, homozygous deletion of the *Dkk3* gene in mice has only minor effects on blood cell counts, lung ventilation and behaviour, with no reported increase in mortality or spontaneous tumor formation (del Barco Barrantes et al., 2006; Papatriantafyllou et al., 2012). A clue to the possible role of Dkk-3 in normal tissues comes from siRNA studies in prostate epithelial cells, where Dkk-3 expression is required for formation of acini in three-dimensional (3D) Matrigel cultures (Kawano et al., 2006).

Ectopic expression of Dkk-3 in cells has effects on several signalling pathways. There are conflicting reports on whether and how Dkk-3 affects Wnt/β-catenin signalling (Hoang et al., 2004; Lee et al., 2009; Ueno et al., 2011; Yue et al., 2008). Wnt/β-catenin signalling, which plays complex roles in prostate cancer (Kypta and Waxman, 2012), is initiated by Wnt ligand binding to Frizzled and LRP5/6 receptors, leading to β-catenin stabilization (Clevers, 2006). Dkk-1, -2 and -4 inhibit Wnt/β-catenin signals by binding to LRP5/6 (Niehrs, 2006), but Dkk-3 does not bind to these proteins directly (Mao and Niehrs, 2003; Mao et al., 2001). Instead, Dkk-3 has been reported to affect Wnt signalling through binding other proteins, namely Kremen1/2 (Nakamura and Hackam, 2010), β-TrcP (Lee et al., 2009) and TcTex-1 (Ochiai et al., 2011). However, Dkk-3 is a secreted protein and the relevance of these interactions, which take place in the cytoplasm, to the function of endogenous Dkk-3 remains unclear. In addition, ectopic expression of Dkk-3 affects the activities of several kinases, including JNK, p38, and Erk (Abarzua et al., 2005; Gu et al., 2011; Hsu et al., 2011), but it is not known if secreted Dkk-3 has similar effects. Studies performed in *Xenopus* and zebrafish embryos highlight a functional link between Dkk-3 and TGF-β signalling. When TGF-β ligands bind their receptor complexes, they phosphorylate Smad2 and Smad3, which then interact with Smad4 and

translocate to the nucleus to regulate gene expression (Massagué, 2008). Dkk-3 stabilization of Smad4 is required for mesoderm induction in *Xenopus* embryos (Pinho and Niehrs, 2007), and Dkk-3 maintains Smad4 levels in zebrafish embryos to enable myogenic differentiation (Hsu et al., 2011). In addition, Dkk-3 inhibits both Wnt/β-catenin and Nodal/Vg1 signalling pathways in the basal chordate Amphioxus (Onai et al., 2012), and overexpression of Dkk-3 in malignant mesothelioma cells increases Smad3 and downregulates ID1 expression in a manner that requires both Smad and ATF3 binding to the ID1 promoter (Kashiwakura et al., 2008).

Here, we have analysed prostate gland morphology in *Dkk3*-null mice and studied the signals regulated by endogenous Dkk-3 in human prostate epithelial cells. We find that loss of Dkk-3 affects prostate cell proliferation *in vivo* and *in vitro* in 3D cultures, and we provide evidence that Dkk-3-dependent acinar morphogenesis requires inhibition of TGF-β/Smad signalling. Our results suggest that endogenous Dkk-3 controls the response to TGF-β, and thus its loss in cancer may play a role in the TGF-β signalling switch from tumor suppression to tumor promotion.

Results

Prostate epithelial cell proliferation is increased in Dkk-3-null mice

Dkk3-null mice are viable and fertile and do not show any major morphological or phenotypic alterations (del Barco Barrantes et al., 2006). To determine whether Dkk-3 affects prostate development, prostate samples were obtained from mice aged 6 and 8 weeks, when prostate development is almost complete (Sugimura et al., 1986). Mitotic cells were observed by Hematoxylin and Eosin staining in Dkk-3 knockout mice but not in wild-type littermates (Fig. 1A). This result suggested that cells in Dkk-3 knockout mice proliferate faster than those in wild-type littermates. To confirm this, prostates from these mice were stained with anti-Ki-67 antibody in order to analyse the proliferation potential of cells. Compared to wild-type mice, the Ki-67 labelling index in the prostates of Dkk-3 knockout mice is significantly higher in all the prostate lobes (Fig. 1C,D; a cartoon depicting the anatomy of the mouse prostate is shown in supplementary material Fig. S1). In addition, some areas of Dkk-3-null mouse prostates appear disorganized (Fig. 1A), as also
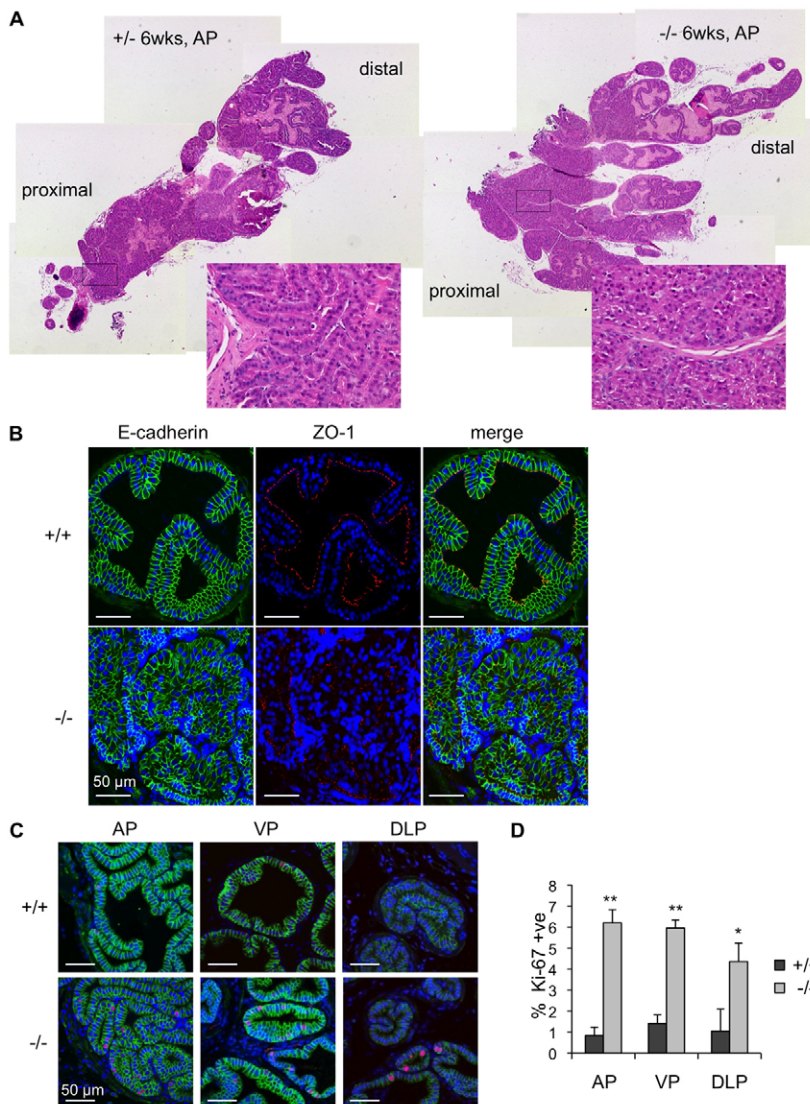
Fig. 1. Increased cell proliferation *in vivo* in Dkk-3-null mouse prostate epithelium. (**A**) Haematoxylin and Eosin staining of sections of anterior prostate (AP) from heterozygous and *Dkk3*-null mice at 6 weeks (40× magnification). The boxed areas are magnified to show a disorganized region in *Dkk3* mutant mouse prostate in more detail (200×). (**B**) Immunohistochemistry for E-Cadherin (green) and ZO-1 (red) on sections of the dorsal prostate. Nuclei were stained with TO-PRO-3 (blue). (**C**) Immunohistochemistry for E-Cadherin (green) and Ki-67 (red) on sections of the dorsal (AP), ventral (VP) and dorsolateral (DLP) prostate. Nuclei were stained with TO-PRO-3 (blue). (**D**) Quantitative analysis of Ki-67-positive prostate epithelial cells (E-Cadherin-positive) in each lobe of wild-type and *Dkk3* knockout mice. The number of Ki-67-positive cells was significantly higher in all lobes of *Dkk3*-null prostates ($n=3$), compared with controls ($n=3$). Student's *t*-test: *$P<0.05$, **$P<0.001$.

observed by immunofluorescence staining, which revealed misalignment of the tight junction component ZO-1 (Fig. 1B).

Loss of Dkk-3 increases proliferation of human prostate epithelial cells cultured as acini but not as monolayers

In order to examine the role of Dkk-3 in more detail, we established a cell culture model using RWPE-1, a non-malignant immortalized human prostatic epithelial cell line that is used as a physiologically relevant system for the regulation of growth, morphogenesis and differentiation in the normal human prostate (Kawano et al., 2006; Webber et al., 1997; Webber et al., 2001). RWPE-1 cells are immortalized by human papillomavirus 18, retain expression of luminal epithelial cell markers, such as cytokeratin 8 and 18 (Webber et al., 1997), and have the ability to form acini with a hollow lumen when grown in 3D Matrigel cultures (Bello-DeOcampo et al., 2001a), a feature that is not manifested by LNCaP (Härmä et al., 2010) or DU145 (Bello-DeOcampo et al., 2001b) prostate cancer cell lines. RWPE-1 cell sublines were established that expressed a microRNA-adapted shRNA (shRNAmir) targeting Dkk-3. Quantitative real-time PCR (qRT-PCR) and western blot analysis showed that cells stably transfected with control shRNAmir [non-silenced (NS) clones] expressed levels of Dkk-3 comparable to parental cells, while cells stably transfected with Dkk-3 shRNAmir (sh clones) expressed very little Dkk-3 (Fig. 2A,B); *DKK3* mRNA levels in clones sh6 and sh30 were 3.6% and 11.2%, respectively, of the level in clone NS11. RWPE-1 cells contain subpopulations of stem/progenitor cells that express different levels of differentiation markers, including p63 and cytokeratin 14 (CK14) (Tokar et al., 2005). Western blotting analysis indicated that the control and Dkk-3-silenced cell lines expressed similar levels of p63 and CK14 as parental cells (supplementary material Fig. S2A), indicating that we had not selected clones with different stem/progenitor-like properties.

In order to examine the effect of Dkk-3 silencing on cell proliferation, cells were plated on untreated glass slides or slides pre-coated with Matrigel and assayed for BrdU incorporation. No significant differences in proliferation were observed among the cell lines, whether cultured on glass or Matrigel (Fig. 2C). In addition, silencing of Dkk-3 did not appear to affect the

cytoskeleton, as measured by localization of β-catenin and F-actin (supplementary material Fig. S2B). These results indicate that Dkk-3 silencing does not detectably affect RWPE-1 cell proliferation or morphology in monolayer cultures.

To examine the effect of Dkk-3 depletion on cells cultured in 3D, we performed acinar morphogenesis assays in Matrigel. Three different phenotypes were observed in RWPE-1 cells undergoing acinar morphogenesis, which we defined as normal (polarized spherical structures), notched (slightly disrupted spheres) and deformed (irregular non-spherical structures) (supplementary material Fig. S3). Dkk-3-depleted cells started to manifest a deformed phenotype at day 6, and this became more apparent on day 7 (Fig. 3A), confirming our previous observations using Dkk-3 siRNA oligonucleotides (Kawano et al., 2006). Given the technical difficulties of performing BrdU incorporation assays under these experimental conditions, proliferation was estimated by measuring phosphorylation of histone-H3 (PH3). Compared with controls, there were significantly more PH3-positive cells in acini formed by Dkk-3-silenced cells (Fig. 3B). In contrast, there were no significant differences in the numbers of apoptotic cells, as measured by immunostaining for cleaved caspase 3 (Fig. 3B), suggesting that loss of Dkk-3 does not affect apoptosis under these culture conditions. Taken together, these results suggest that Dkk-3 has a pleiotropic role during acinar morphogenesis, namely, controlling cell proliferation and spherically-arranged polarization.

Recombinant Dkk-3 partially rescues the acinar morphogenesis phenotype in Dkk-3-silenced cells

Although Dkk-3 is a secreted protein, there are reports suggesting that it can function intracellularly (Lee et al., 2009; Nakamura and Hackam, 2010). To determine if extracellular Dkk-3 is sufficient to restore normal acinar morphogenesis, we supplemented the media with recombinant Dkk-3 (Fig. 3C). Dkk-3 (10 μg/ml) significantly reduced the number of deformed acini formed by Dkk-3-silenced cells ($P=0.005$) and increased the numbers of normal and notched acini ($P=0.002$). Interestingly, Dkk-3 also reduced the number of normal acini formed by control cells. Lower concentrations of Dkk-3 (0.1 and 1 μg/ml) did not induce significant changes in acini formed by
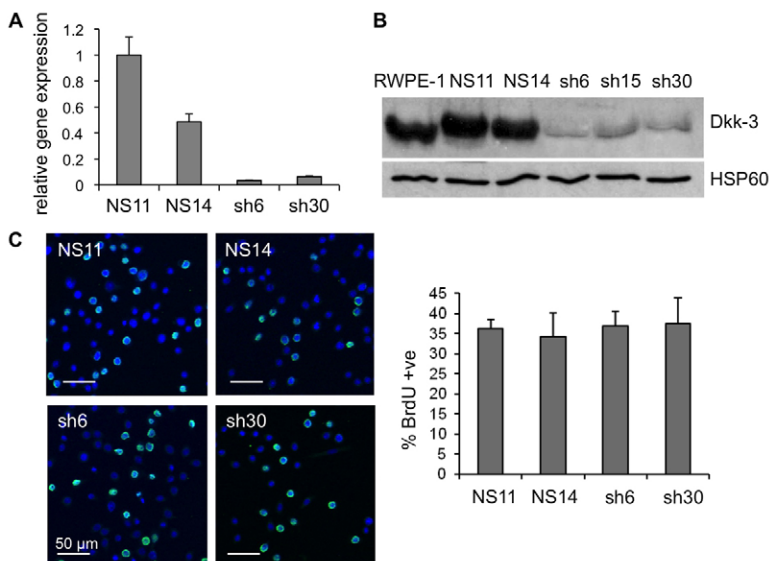

Fig. 2. Characterisation of RWPE-1 lines depleted of Dkk-3. (**A**) Quantitative PCR and (**B**) western blot analysis of *DKK3* mRNA and Dkk-3 protein levels in Dkk-3 shRNA (sh6 and sh30) and control shRNA (NS11 and NS14) RWPE-1 sublines. (**C**) BrdU (green) and nuclear (TO-PRO-3, blue) staining in RWPE-1 sublines cultured as monolayers. The average and s.d. of the percentage of BrdU-positive cells are shown (*n*=5 fields). Statistical analysis revealed that there is no significant difference in the percentage of BrdU-positive cells ($P=0.33$ Student's *t*-test for NS14 vs sh30).
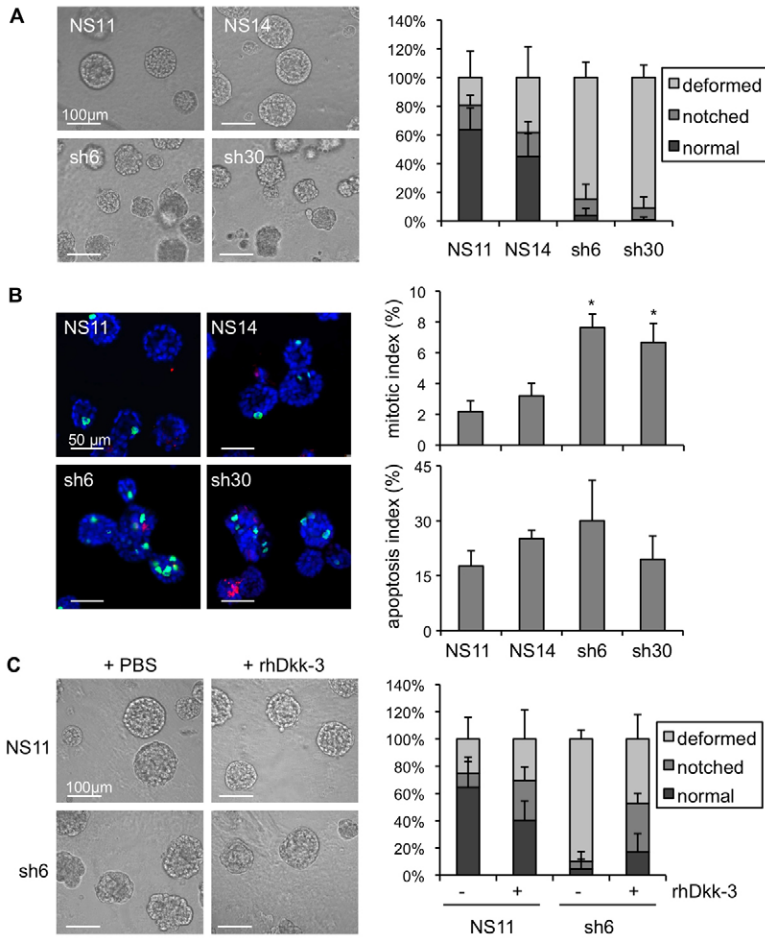
Fig. 3. Increased cell proliferation in Dkk-3-depleted cells cultured in 3D. (**A**) Effect of Dkk-3 expression in RWPE-1 cells in prostate acinar morphogenesis assay. 5000 cells per well were prepared in assay medium and plated on Matrigel-coated 8-well chamber glass slides. Images were taken at different timepoints; those shown are after 8 days in 3D culture. At least 100 acini per sample were scored. The bar chart shows the average and s.d. in six fields per sample. The number of normal acini was significantly lower in Dkk-3 shRNA sublines compared with the control shRNA sublines (Student's t-test: NS11 vs sh6 $P=0.031$, and NS11 vs sh30 $P=0.002$). (**B**) Immunocytochemistry for the detection of phospho-histone H3 (as a marker of cell proliferation; green) and cleaved caspase 3 (as a marker of apoptosis; red) in acini at 5 days. The average and s.d. of the percentage of phospho-histone-H3-positive, and cleaved caspase-3-positive cells are shown ($n=$five fields), *$P<0.05$, Student's t-test. (**C**) Treatment with recombinant Dkk-3 partially rescues the defective acinar morphogenesis phenotype in Dkk-3 shRNA sh6 cells. The images shown were taken after 9 days in 3D culture. Quantification was performed as described for A.

sh6 cells or by control NS11 cells (data not shown). Taken together, these results indicate that acinar morphogenesis requires optimal expression and/or localization of Dkk-3.

Loss of Dkk-3 increases TGF-β/Smad signalling in prostate epithelial cells

To further clarify the role of Dkk-3 in acinar morphogenesis, we sought to determine the effects of Dkk-3 depletion on signalling pathways implicated in the response to Dkk-3. In light of reports that Dkk-3 affects Wnt/β-catenin signalling, we first analysed β-catenin/Tcf transcriptional activity using the Super8×TOPFlash luciferase reporter (Veeman et al., 2003). Under basal conditions, Wnt/β-catenin activity was similar in all the cell clones (Fig. 4A). Comparison with the activity of Super8×FOPflash, a reporter in which the Tcf binding sites are mutated, indicated that basal Wnt/β-catenin signalling activity is very low in RWPE-1 cells, both in the presence and absence of Dkk-3 [the TOPFlash/FOPFlash ratio is 0.5 in RWPE-1 cells, whereas it is >10 in colon cancer cell lines (Giannini et al., 2000)]. We also examined expression of the Wnt/β-catenin target genes *AXIN2*, *NKD1*, *DKK1* and *MYC*. *AXIN2* expression was below the limit of detection [cycle threshold (Ct) values >33, results not shown], *NKD1* expression was also low (Ct >27) and not affected by the Wnt signalling inhibitor IWP-2 (Fig. 4B), and expression of *MYC* and *DKK1* was high (Ct <21) but unaffected by IWP-2, suggesting that these two genes are regulated by Wnt-independent

signals in RWPE-1 cells. Silencing of Dkk-3 did not increase the expression of these genes (Fig. 4B), suggesting that loss of Dkk-3 does not lead to activation of Wnt/β-catenin signalling. However, co-transfection of a small amount of β-catenin expression plasmid increased β-catenin/Tcf activity in Dkk-3-silenced cells, relative to control cells (Fig. 4A), suggesting that once activated, Wnt/β-catenin signalling can be potentiated upon loss of Dkk-3. Consistent with this, co-transfection of a Dkk-3 plasmid with β-catenin in Dkk-3-silenced cells inhibited β-catenin/Tcf activity (Fig. 4C).

Since the effects of Dkk-3 on cell growth were observed only in 3D cultures, we hypothesized that Wnt/β-catenin signalling might become activated in 3D cultures and further activated upon silencing of Dkk-3. However, comparison of Wnt target gene expression in control (NS11) 3D cultures indicated that Wnt/β-catenin signalling is not activated under these conditions, since *AXIN2* remained undetectable (data not shown), *MYC* expression was lower and *NKD1* expression was unchanged (Fig. 4D). Moreover, 3D cultures of Dkk-3-silenced cells (sh6) showed no significant increase in *NKD1*, *MYC* or *AXIN2* expression, compared with 2D cultures. Together, these results suggest that the effects of Dkk-3 on acinar morphogenesis are unlikely to involve Wnt/β-catenin signalling.

We noted that *DKK1* expression was increased in 3D cultures of NS11 cells but not in sh6 cells, suggesting that Dkk-3 regulates a Wnt/β-catenin-independent signal in 3D cultures that leads to
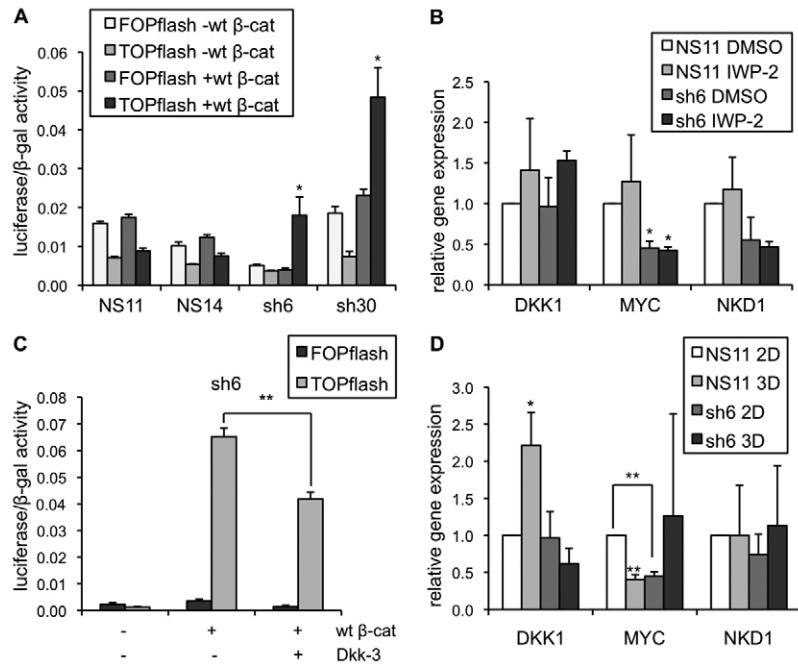
Fig. 4. Effects of Dkk-3 on Wnt/β-catenin signalling in RWPE-1 cells. (**A**) Gene reporter assays were carried out in RWPE-1 sublines transfected with Super8×TOPflash or Super8×FOPflash, pDM-β-gal, pcDNA or pcDNA β-catenin (wild type, wt); *$P<0.001$ for TOPflash +wt β-cat in sh6 and sh30 vs NS11 cells, Student's t test, $n=3$. (**B**) The expression of the Wnt/β-catenin target genes *DKK1*, *MYC* and *NKD1* were analysed by q-PCR in the indicated RWPE-1 sublines, as described in the Materials and Methods; *$P<0.05$, Student's t-test for *MYC* NS11 vs sh6 in 2D, $n=2$. (**C**) Gene reporter assays from RWPE-1 sh6 cells transfected with Super8×TOPflash or Super8×FOPflash, pDM-β-gal, empty vector, β-catenin and Dkk-3 as indicated; **$P<0.05$, Student's t-test, $n=3$. (**D**) *DKK1*, *MYC* and *NKD1* were analyzed by qPCR as described for B. Independent experiments were performed in triplicate (*DKK1* and *MYC*, $n=3$; *NKD1*, $n=5$); *$P<0.05$ for 2D vs 3D, **$P<0.001$ for NS11 2D vs sh6 2D.

increased *DKK1* expression. Since TGF-β1 has been reported to affect *DKK1* expression (Akhmetshina et al., 2012; Kane et al., 2008) and to inhibit acinar morphogenesis (Tyson et al., 2007), we investigated the effect of Dkk-3 depletion on TGF-β signalling. We first examined Smad2 and Smad3, which are phosphorylated upon TGF-β receptor activation. TGF-β1 increased Smad2 phosphorylation to a greater extent in Dkk-3-silenced cells than in control cells (Fig. 5A), suggesting that silencing of Dkk-3 increases TGF-β/Smad signalling. There were no significant differences in the expression or phosphorylation of other Smad proteins in control and Dkk-3-silenced cells (supplementary material Fig. S4). Next, TGF-β1/Smad-dependent transcriptional activity was measured using CAGA12, a luciferase reporter that contains Smad binding

elements (Dennler et al., 1998). Basal CAGA12-luciferase activity was higher in Dkk-3-depleted cell clones than in control clones (Fig. 5B). In addition, TGF-β1-stimulated activity was higher in sh6 cells, which express the lowest level of Dkk-3, suggesting that endogenous Dkk-3 inhibits TGF-β/Smad signalling. In support of this, transfection of Dkk-3 plasmid inhibited TGF-β1-stimulated CAGA12-luciferase activity in sh6 cells (Fig. 5C).

In order to determine if loss of Dkk-3 affects TGF-β/Smad signalling during acinar morphogenesis, we examined the expression of *PMEPA1*, a TGF-β/Smad target gene that is known to play a role in RWPE-1 cell proliferation (Liu et al., 2011). Expression of *PMEPA1* was reduced by SB431542, a specific TGF-β receptor inhibitor (Matsuyama et al., 2003),
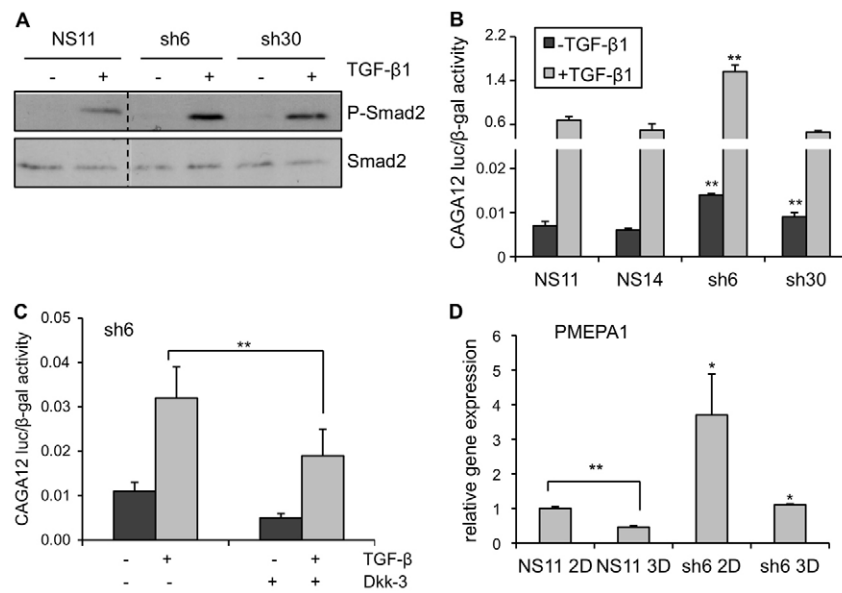

Fig. 5. Dkk-3 depletion increases TGF-β1/Smad signalling in RWPE-1 cells. (**A**) Extracts from the indicated RWPE-1 sublines treated for 1 h with vehicle (PBS) or 1 ng/ml TGF-β1 were blotted for P-Smad2 and Smad2. (**B**) Gene reporter assays were carried out in RWPE-1 sublines transfected with pGL3-CAGA12-luciferase and pDM-β-gal. After 3 h, 1 ng/ml TGF-β1 or an equivalent volume of vehicle (PBS) was added to the cells for an additional 21 h; **$P<0.001$ vs NS11, Student's t-test $n=3$. (**C**) Gene reporter assays were carried out in RWPE-1 sh6 cells transfected with pGL3-CAGA12-luciferase, pDM-β-gal and empty vector or Dkk-3. After 3 h, 1 ng/ml TGF-β1 or an equivalent volume of vehicle (PBS) was added to the cells for an additional 21 h; **$P<0.05$, Student's t-test, $n=2$. (**D**) The expression of *PMEPA1* was analyzed by q-PCR in RWPE-1 cells growing as a monolayer (2D) or during acinar morphogenesis (3D), as described in the Materials and Methods; * $P<0.05$ for NS11 2D vs sh6 2D, NS11 3D vs sh6 3D; **$P<0.01$ for NS11 2D vs NS11 3D, Student's t-test, $n=4$.

confirming that this gene is regulated by TGF-β in RWPE-1 cells (see Fig. 6B). In addition, *PMEPA1* expression was lower in 3D cultures than in 2D cultures (Fig. 5D), suggesting that it is downregulated during acinar morphogenesis. Finally, *PMEPA1* expression was higher in sh6 cells than in NS11 cells, suggesting that Dkk-3 normally negatively regulates *PMEPA1* expression. Taken together, these results support the possibility that Dkk-3 limits TGF-β/Smad signalling during acinar morphogenesis.

Inhibition of TGF-β signalling, but not Wnt signalling, rescues the defective acinar phenotype in Dkk-3-depleted cells

In order to determine if the effects of Dkk-3 on TGF-β/Smad signalling are relevant to acinar morphogenesis, we studied the effects of the TGF-β receptor inhibitor SB431542. Addition of SB431542 to the cell culture media significantly increased the number of normal acini formed by Dkk-3-silenced cells ($P=0.001$ for sh6 + DMSO versus sh6 + 1 μM SB431542; Fig. 6A). The same result was observed using sh30 cells (results not shown). In contrast, SB431542 had no significant effect on

the number of normal acini formed by control cells ($P=0.385$, NS11 + DMSO versus NS11 + 1 μM SB431542). As expected, SB431542 inhibited TGF-β1-induced CAGA12 reporter activity in 2D cultures (supplementary material Fig. S5B) and inhibited TGF-β/Smad signalling in 3D cultures, as measured by expression of *PMEPA1* (Fig. 6B). SB431542 did not restore *DKK3* expression in sh6 cells (Fig. 6B), indicating that its ability to rescue acinar morphogenesis did not result from upregulation of *DKK3* expression. To determine if the rescue of acinar morphogenesis by SB431542 is accompanied by a change in cell proliferation, acini were immunostained for phosphorylated histone H3. The results indicate that SB431542 treatment reduced proliferation of Dkk-3-silenced cells during acinar morphogenesis (Fig. 6C). This is in contrast to cells cultured in 2D, where TGF-β inhibited proliferation (supplementary material Fig. S5A).

In order to confirm that inhibition TGF-β/Smad signalling rescues the defective acinar morphogenesis phenotype in Dkk-3-silenced cells, we used SIS3, a pharmacological inhibitor of Smad3 (Jinnin et al., 2006) and recombinant human TGF-βRII-Fc, a
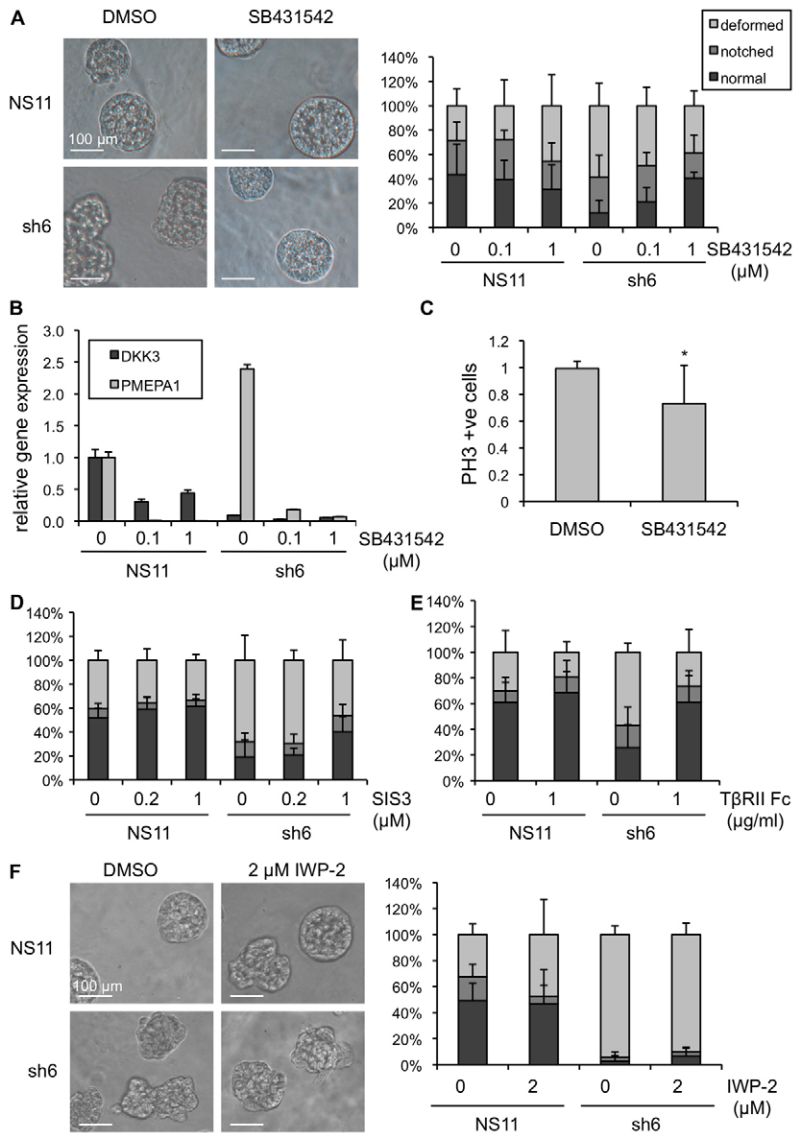
Fig. 6. Inhibition of TGF-β signalling rescues acinar morphogenesis in Dkk-3-depleted RWPE-1 cells. (**A**) Effect of SB431542 on prostate acinar morphogenesis. Acinar morphogenesis assays were carried out in the presence of 0.1 μM SB431542, 1 μM SB431542 or an equivalent volume of vehicle (DMSO). Images were taken after 8 days; images shown are for 1 μM SB431542. Normal, notched and deformed acini were scored as described for Fig. 3A. The chart shows the average and s.d. in six fields per sample. At least 50 acini per sample were scored. (**B**) Quantitative PCR was used to compare the expression of *DKK3* and *PMEPA1* using RNA from acini after 8 days in 3D culture, treated as indicated. Each gene was analyzed in triplicate in at least two independent experiments. (**C**) Effects of SB431542 on proliferation in acini. Acini formed at 5 days were immunostained for phospho-histone H3, as for Fig. 3B. Graph shows relative number of PH3-positive cells in acini treated with 1 μM SB431542, compared with acini treated with DMSO; $n=2$, duplicate assays counting >5 fields per sample; *$P<0.05$, Student's t-test. (**D**) Effects of SIS3 on prostate acinar morphogenesis. Acinar morphogenesis assays were carried out in the presence of 0.2 μM SIS3, 1 μM SIS3 or an equivalent volume of vehicle (DMSO) and images were taken after 8 days; representative images for 1 μM SIS3 are shown in supplementary material Fig. S5E. Normal, notched and deformed acini were scored and plotted as for panel A. (**E**) Effects of TGFβRII-Fc on prostate acinar morphogenesis. Acinar morphogenesis assays were carried out in the presence of 1 μg/ml TGFβRII-Fc or an equivalent volume of vehicle (PBS) and images were taken after 6 days; representative images are shown in supplementary material Fig. S5F. Normal, notched and deformed acini were scored and plotted as for A. (**F**) Effects of inhibition of Wnt signalling on prostate acinar morphogenesis. Acinar morphogenesis assay were carried out in the presence of 2 μM IWP-2 or an equivalent volume of vehicle (DMSO) and images were taken after 7 days. Normal, notched and deformed acini were scored and plotted as for A.

soluble decoy receptor that blocks binding of TGF-β ligands to its cognate receptors. TGF-βRII-Fc inhibited TGF-β/Smad signalling as effectively as SB431542 both when tested in CAGA-luciferase assays (supplementary material Fig. S5B) and when tested for its effects on PMEPA1 expression in RWPE-1 sh6 cell acini (supplementary material Fig. S5D). In contrast, SIS3 inhibited TGF-β activation of CAGA-luciferase activity only weakly (supplementary material Fig. S5B). However, it was able to inhibit endogenous PMEPA1 expression in monolayer cultures (supplementary material Fig. S5C). Consistent with these results, SIS3 only partially rescued the acinar morphogenesis phenotype in Dkk-3-silenced cells (Fig. 6D and supplementary material Fig. S5E), whereas acinar morphogenesis was completely rescued by TGF-βRII-Fc (Fig. 6E and supplementary material Fig. S5F). Finally, we examined the effect of the Wnt inhibitor IWP-2 (Chen et al., 2009a) on acinar morphogenesis. IWP-2 had a small negative effect on acinar morphogenesis in control clones and slightly increased the proportion of normal acini in Dkk-3-silenced cells, although this was not statistically significant (Fig. 6F). Taken together, these results indicate that Dkk-3 promotes normal acinar morphogenesis by limiting TGF-β signalling, rather than Wnt signalling.

Discussion

A potential role for Dkk-3 in the structural integrity of the prostate was first suggested from *in vitro* studies of prostate epithelial cells cultured in 3D (Kawano et al., 2006). In this report, we provide the first *in vivo* evidence to support this hypothesis. Histological analysis revealed areas of *Dkk3*-null mouse prostates where the epithelium was no longer organized as a monolayer structure. This is characteristically observed in high Gleason score prostate cancer, supporting our previous findings that loss of Dkk-3 expression correlates with high Gleason score (Kawano et al., 2006). However, since this phenotype was not observed in all *Dkk3*-null mice, additional studies using mice at different ages will be required to determine if the phenotype is transient and/or if it leads to more dramatic changes in the prostates of older mice. What was observed in all *Dkk3*-null mice, however, is an increase in prostate epithelial cell proliferation, compared to in wild-type littermates. Despite the increased numbers of proliferating cells, we did not observe an increase in prostate size in Dkk-3-null mice. Prostate size also does not increase in Nkx3.1 mutant mice at 6 weeks, despite an increase in the number of Ki67-positive cells (Bhatia-Gaur et al., 1999). More detailed studies of Dkk-3 mutant mouse prostates will be required to determine the long-term consequences of the increase in proliferation. Importantly, we also observed increased proliferation in human prostate epithelial cells depleted of Dkk-3, suggesting that Dkk-3 mutant mice may provide a useful *in vivo* model for studying the function of Dkk-3 in the prostate and in prostate cancer.

The disruption of acinar morphogenesis that occurs upon loss of Dkk-3 could result from effects on apoptosis, which is required for lumen formation in acini (Debnath et al., 2002). However, we did not observe differences in the numbers of apoptotic cells in control and Dkk-3-silenced acini. Moreover, although ectopic expression of Dkk-3 induces cancer cell apoptosis (Veeck and Dahl, 2012), we are not aware of any reports that silencing of Dkk-3 prevents apoptosis. In fact, silencing of Dkk-3 in growth-arrested fibroblasts leads to apoptosis (Tudzarova et al., 2010). Our results therefore favour a model in which increased cell

proliferation accounts for the phenotypes observed upon loss of Dkk-3 in mice and in 3D cultures. Among the genes that we analysed, the *MYC* gene product is most directly involved in cell proliferation. Interestingly, *MYC* expression levels were lower in control RWPE-1 cells cultured in 3D, compared to in 2D (Fig. 4D), and this reduction was not observed in Dkk-3-depleted cells, further supporting a role for Dkk-3 in the control of cell proliferation in 3D cultures.

Addition of recombinant Dkk-3 only partially rescued the acinar morphogenesis phenotype in Dkk-3-silenced cells. It is possible that purified Dkk-3 is only partially active, as there are no specific assays to measure its activity. However, we obtained similar results using a commercial source of Dkk-3 and native untagged Dkk-3 purified from prostate cells (Zenzmaier et al., 2008). A plausible explanation for the partial rescue is that the cells responding to Dkk-3 are located inside acini and have limited access to exogenously applied Dkk-3 protein. Alternatively, or in addition, Dkk-3 may need to be presented to cells in acini in a polarised manner. This would be consistent with the negative effects of purified Dkk-3 on acinar morphogenesis in normal cells.

Wnt/β-catenin signalling activity in monolayer cultures, measured using gene reporter assays and expression of Wnt/β-catenin target genes, was very low in RWPE-1 cells, and elevation of Wnt/β-catenin signalling upon Dkk-3-silencing was only detected upon co-expression of β-catenin. In addition, culture of cells in 3D did not increase expression of Wnt/β-catenin target genes, and the Wnt inhibitor IWP-2 had minimal effects on target gene expression and did not rescue acinar morphogenesis in Dkk-3-silenced cells. We conclude, therefore, that activation of Wnt/β-catenin signalling is unlikely to account for the acinar morphogenesis phenotype observed in Dkk-3-silenced cells.

Rather, our results suggest that loss of Dkk-3 disrupts acinar morphogenesis by activating TGF-β/Smad signalling. A change in the cellular response to TGF-β is frequently observed in cancer, and there is great interest in the molecular mechanisms responsible for the switch of TGF-β signalling from tumor suppression to tumor promotion (Bierie and Moses, 2006; Inman, 2011). TGF-β1 inhibits proliferation of RWPE-1 cells (Bello et al., 1997) and BPH-1 benign prostate epithelial cells (Ao et al., 2006), but does not affect proliferation of metastatic PC3 cells or transformed derivatives of BPH-1, where instead it promotes an epithelial-to-mesenchymal transition (Ao et al., 2006; Zhang et al., 2009). An important TGF-β target gene, *PMEPA1*, has been implicated in this TGF-β switch (Singha et al., 2010), and silencing of *PMEPA1* has been shown to reduce RWPE-1 cell proliferation (Liu et al., 2011). Our results show that *PMEPA1* expression falls during acinar morphogenesis and that it is elevated in Dkk-3-depleted cells, consistent with a model in which loss of Dkk-3 disrupts acinar morphogenesis through TGF-β signalling. Additional studies will be required to determine if the disruption of acinar morphogenesis upon loss of Dkk-3 is mediated by *PMEPA1*, and if this plays a role in the switch of TGF-β from tumor-suppressor to tumor-promoter. Importantly, the ability of SB431542 to rescue acinar morphogenesis in Dkk-3-silenced cells provides further support for the development of TGF-β receptor inhibitors in the treatment of prostate cancer (Jones et al., 2009). SB431542 and TGF-βRII-Fc efficiently rescued the acinar morphogenesis phenotype in Dkk-3-silenced cells, but SIS3 was less effective. Although possible toxicity of

SIS3 cannot be ruled out, the difference might also be related to Smad2 playing a more important role than Smad3 in Dkk-3-silenced cells, as reflected by their differential TGF-β-induced phosphorylation.

The observation that loss of Dkk-3 leads to both increased proliferation and increased TGF-β signalling seems at odds with the fact that TGF-β signalling normally inhibits epithelial cell proliferation. However, TGF-β elicits a variety of complex responses and its impact on proliferation is context-dependent. For example, TGF-β reduces breast cancer cell proliferation in 2D cultures, but increases it *in vivo* (Tobin et al., 2002). We found that TGF-β reduced RWPE-1 cell proliferation and that silencing of Dkk-3 did not affect this response in 2D cultures. In contrast, in 3D cultures silencing of Dkk-3 increased proliferation and inhibition of TGF-β signalling by SB431542 reduced proliferation. Thus, our results suggest that the 3D context changes the proliferative response to TGF-β. Interestingly, EGF prevents inhibition of proliferation by TGF-β in the proximal prostate of the rat (Salm et al., 2005). Since EGF is required for acinar morphogenesis of RWPE-1 cells (Tyson et al., 2007), it is possible that EGF signalling plays a role in the proliferative response to TGF-β in 3D cultures. Taken together, our results suggest that Dkk-3 plays a role in regulating cell-cell interactions in 3D that impact on TGF-β/Smad signalling, and that this may be important for maintaining the structural integrity of the prostate. The identification of Dkk-3 receptors may shed light on how this is achieved.

Materials and Methods

Reagents and antibodies

Human pSM2 retroviral shRNAmir plasmid targeting Dkk-3 (RHS1764-9689535) and Non-silencing shRNAmir plasmid (RHS1703) were purchased from Open Biosystems (Thermo Scientific, Loughborough, UK). Antibodies used recognized Ki-67 (ab15580) from Abcam (Cambridge, UK), ZO-1 from Invitrogen (Life Technologies, Paisley UK), E-Cadherin (610181) and β-catenin (610153) from BD Transduction Labs (Oxford, UK), Dkk-3 (H-130) and GAPDH (2D4A7) from Santa Cruz Biotechnology (Insight Biotechnology, Wembley UK), HSP60 (mouse monoclonal) from Stressgen (Exeter, UK), cleaved caspase 3 (9661) and Smad2, phospho-Smad2, Smad4, phospho-Smad1/5, Smad1, Smad5 and Smad6 (phospho-Smad sampler kit 9963) from Cell Signaling Technologies (New England Biolabs, Hitchin, UK), phospho-Smad3 (AB3226) from R&D systems (Abingdon, UK), Smad3 (EP568Y), p63 (rabbit polyclonal) and phospho-histone H3 Ser10 (3H10) from Millipore (Watford, UK) and CK14 from Abd Serotec (Kidlington, UK). The Alexa Fluor® 488 goat anti-mouse IgG (H⁺L), Alexa Fluor® 555 goat anti-rabbit IgG (H⁺L) antibodies, Alexa Fluor® 555 phalloidin and TO-PRO-3 were from Invitrogen. Recombinant human TGF-β1 and TβRII Fc were from R&D systems. Recombinant human Dkk-3 was from R&D systems and also provided by Peter Berger and Christoph Zenzmaier, Institute for Biomedical Aging Research, Innsbruck, Austria (Zenzmaier et al., 2008). SB431542 and SIS3 were from Sigma (Gillingham, UK), and IWP-2 was from Calbiochem (Merck, Darmstadt, Germany).

Mouse prostate histology and immunohistochemistry

The details of mice deficient for Dkk-3 were described previously (del Barco Barrantes et al., 2006). Analyses were performed using male mice aged 6 and 8 weeks. The histological phenotype of Dkk-3-null mice and wild-type littermate prostates was assessed on Haematoxylin- and Eosin-stained sections, based on published guidelines (Shappell et al., 2004) and assisted by a pathologist (M.M.W.). Serial sections were then stained for immunohistochemical analysis. Antibody staining was carried out on paraffin sections, according to the previously reported method (Francis et al., 2010). Immunofluorescence staining and image acquisition using a confocal microscope were carried out as described below.

Cell culture

RWPE-1 cells were cultured as previously described (Kawano et al., 2006). For establishing Dkk-3 silenced RWPE-1 cells, RWPE-1 cells were transfected with shRNAmir targeting Dkk-3 or non-silencing shRNAmir using Fugene HD (Roche Applied Science, Burgess Hill, UK) according to the manufacturer's instructions, then selected with 0.75 µg/ml puromycin (Sigma). Colonies were expanded,

Dkk-3 expression was determined by western blotting and RT-PCR and clones with efficient Dkk-3 silencing were selected for further analysis.

Western blotting

Western blotting was performed as described previously (Mazor et al., 2004). In brief, for total cell extracts, cells were rinsed in cold PBS and lysed in modified radioimmunoprecipitation assay (RIPA) lysis buffer (0.5% deoxycholate, 1% Triton X-100, 20 mM Tris pH 8.0, 0.1% SDS, 100 mM NaCl, 50 mM NaF, 1 mM EDTA), with a cocktail of protease inhibitors (Roche). To detect endogenous Dkk-3, the culture supernatant from cells in six-well plates was centrifuged to remove cell debris and added to 10 µl StrataClean Resin (Stratagene, Stockport, UK). Resin-bound proteins were pelleted by centrifugation and resuspended in SDS sample buffer. Equal protein loading was confirmed by blotting for HSP60 or GAPDH. A phosphatase inhibitor cocktail (Roche) was added to the lysis buffer in experiments carried out to detect phosphorylated proteins.

RNA analysis

Total RNA from cultured cells was extracted using RNeasy mini kit according to the manufacturer's instructions (Qiagen, Crawley, UK), and reverse transcription was done using Superscript II (Invitrogen) and 3 µg of total RNA from cultured cells. Alternatively, reverse transcription was performed on 1 ug of total RNA using M-MLV Reverse Transcriptase and RNase OUT Ribonuclease Inhibitor (Invitrogen) according to manufacturer's instructions. For analysis of RNA samples from cells grown in 3D, acini were pelleted as described in by Lee et al. (Lee et al., 2007) with modifications. Briefly, the cells were rinsed with ice-cold PBS. PBS/5 mM EDTA was added to the cell culture surface and the Matrigel was detached from the bottom using a tip. The microwell plates were left on ice on a shaker for 20 min and then the suspensions were transferred to microcentrifuge tubes. The spheres were collected by centrifugation at 1300 rpm for 5 min, washed once with PBS/5 mM EDTA, and then centrifuged again. RNA was extracted from cell pellets using the RNeasy mini kit or PureLink RNA Micro Kit (Invitrogen). Quantitative-PCR was performed using PerfeCTa Sybr Green Supermix, Low Rox (Quanta, Barcelona, Spain) in a Viia7 Real-Time PCR System (Applied Biosystems, Madrid, Spain). Relative fold changes in mRNA were determined according to the ΔΔCt method, relative to the housekeeping gene *36B4*, and intra-experimental standard deviation (s.d.) was calculated according to Bookout and Mangelsdorf (Bookout and Mangelsdorf, 2003). Statistical significance was calculated from three to five independent experiments using Student's *t* test.

Primer sequences

The following primers were used: DKK3 forward 5′-TCATCACCTGGG-AGCTAGAG-3′, DKK3 reverse 5′-TTCATACTCATCGGGGACCT-3′, DKK1 forward 5′-ATGCGTCACGCTATGTGCT-3′, DKK1 reverse 5′-TCTGGAATA-CCCATCCAAGG-3′, AXIN2 forward 5′-AAGTGCAAACTTTCGCCAAC-3′, AXIN2 reverse 5′-ACAGGATCGCTCCTCTTGAA-3′, MYC forward 5′-CA-CCGAGTCGTAGTCGAGGT-3′, MYC reverse 5′-TTTCGGGTAGTGGAAA-ACCA-3′, NKD1 forward 5′-ACTTCCAGCCGAAAGTCGT-3′, NKD1 reverse 5′-CACCATAGGCCGAAGCAC-3′, PMEPA1 forward 5′-CGAGATGGTGGG-TGGCAGGTC-3′, PMEPA1 reverse 5′-CGCACAGTGTCAGGCAACGG-3′, 36B4 forward 5′-GTGTTCGACAATGGCAGCAT-3′ and 36B4 reverse 5′-AGACACTGGCAACATTGCGGA-3′.

Acinar morphogenesis assays

The three-dimensional culture of RWPE-1 cells on Matrigel was carried out according to (Debnath et al., 2003) with minor modifications (Kawano et al., 2006); an illustration of the assay is shown in supplementary material Fig. S3. Briefly, cells were resuspended in keratinocyte serum free medium with 2% calf bovine serum, 5 ng/ml EGF, 2% Matrigel and 0.375 µg/ml puromycin and then plated on Matrigel. When indicated, recombinant proteins or drugs were added to the assay medium at the indicated final concentrations. Images were obtained either using an Axiovert S 100 microscope (Zeiss) and processed by MetaMorph (Molecular Devices) or using an Eclipse TE2000-U microscope (Nikon) and Image-Pro (Media Cybernetics Inc.).

Immunocytochemistry

For 2D culture, RWPE-1 clones were cultured for 2 days on 8-well chamber glass slides pre-coated with Matrigel and then fixed and stained as previously described (Uysal-Onganer et al., 2010). 5-Bromo-2′-deoxyuridine Labeling and Detection Kit II (Roche) was used for BrdU staining to analyse cell proliferation in 2D culture. For 3D culture, fluorescent staining was performed as previously reported by Debnath et al. (Debnath et al., 2003). Nuclei were counterstained using TO-PRO-3 (Invitrogen). Images were acquired on a LSM 510 laser scanning confocal microscope (Zeiss). Mitotic index was determined by calculating the percentage of phospho-histone H3-positive cells (at least 500 cells), and then an average was obtained from triplicate samples. Apoptosis index was determined as previously reported (Guo et al., 2010).

Gene reporter assays

Super8×TOPflash and Super8×FOPflash (Veeman et al., 2003) were kindly provided by Randall Moon (University of Washington, Seattle). Other plasmids used have been described previously (Kawano et al., 2009; Kawano et al., 2006). One million cells per well were plated in 6-well tissue culture plates. After 24 h, cells were transfected with reporter constructs using FuGENE HD (Roche), as described by the manufacturer. For β-catenin/Tcf reporter assays, cells were transfected with 1.55 µg Super8×TOPflash or Super8×FOPflash reporters, 200 ng pDM-β-gal, 50 ng pcDNA β-catenin, 200 ng pcDNA Dkk-3 or the equivalent amounts of empty vector. For TGF-β/Smad reporter assays, cells were transfected with 1.6 µg pGL3-CAGA12-luciferase, 200 ng pDM-β-gal and 200 ng pcDNA Dkk-3, and empty vector (pcDNA3) used to bring the total amount of plasmid to 2 µg per well. Recombinant proteins and/or drugs were added 3 h after transfection when indicated. Luciferase activity was assayed 24 h after transfection using Steadyliteplus (Perkin Elmer). The values obtained were normalized for β-galactosidase activity detected using Galacto-Light Plus (Applied Biosystems, Warrington, UK). Three separate experiments using duplicates were performed in each case.

Author contributions

D.R. and Y.K conceived, designed, conducted and interpreted experiments and wrote the manuscript. N.B. designed, conducted and interpreted experiments, and helped write the manuscript. M.M.W interpreted histology results. N.M. and C.N provided and validated samples for *in vivo* analysis. J.W. helped conceive the study and helped write the manuscript. R.K. conceived the study, designed and interpreted experiments and wrote the manuscript.

Supplementary material available online at
http://jcs.biologists.org/lookup/suppl/doi:10.1242/jcs.119388/-/DC1

References

Abarzua, F., Sakaguchi, M., Takaishi, M., Nasu, Y., Kurose, K., Ebara, S., Miyazaki, M., Namba, M., Kumon, H. and Huh, N. H. (2005). Adenovirus-mediated overexpression of REIC/Dkk-3 selectively induces apoptosis in human prostate cancer cells through activation of c-Jun-NH2-kinase. *Cancer Res.* **65**, 9617-9622.

Akhmetshina, A., Palumbo, K., Dees, C., Bergmann, C., Venalis, P., Zerr, P., Horn, A., Kireva, T., Beyer, C., Zwerina, J. et al. (2012). Activation of canonical Wnt signalling is required for TGF-β-mediated fibrosis. *Nat. Commun.* **3**, 735.

Ao, M., Williams, K., Bhowmick, N. A. and Hayward, S. W. (2006). Transforming growth factor-beta promotes invasion in tumorigenic but not in nontumorigenic human prostatic epithelial cells. *Cancer Res.* **66**, 8007-8016.

Bello, D., Webber, M. M., Kleinman, H. K., Wartinger, D. D. and Rhim, J. S. (1997). Androgen responsive adult human prostatic epithelial cell lines immortalized by human papillomavirus 18. *Carcinogenesis* **18**, 1215-1223.

Bello-DeOcampo, D., Kleinman, H. K., Deocampo, N. D. and Webber, M. M. (2001a). Laminin-1 and alpha6beta1 integrin regulate acinar morphogenesis of normal and malignant human prostate epithelial cells. *Prostate* **46**, 142-153.

Bello-DeOcampo, D., Kleinman, H. K. and Webber, M. M. (2001b). The role of alpha 6 beta 1 integrin and EGF in normal and malignant acinar morphogenesis of human prostatic epithelial cells. *Mutat. Res.* **480-481**, 209-217.

Bhatia-Gaur, R., Donjacour, A. A., Sciavolino, P. J., Kim, M., Desai, N., Young, P., Norton, C. R., Gridley, T., Cardiff, R. D., Cunha, G. R. et al. (1999). Roles for Nkx3.1 in prostate development and cancer. *Genes Dev.* **13**, 966-977.

Bierie, B. and Moses, H. L. (2006). Tumour microenvironment: TGFbeta: the molecular Jekyll and Hyde of cancer. *Nat. Rev. Cancer* **6**, 506-520.

Bookout, A. L. and Mangelsdorf, D. J. (2003). Quantitative real-time PCR protocol for analysis of nuclear receptor signaling pathways. *Nucl. Recept. Signal.* **1**, e012.

Chen, B., Dodge, M. E., Tang, W., Lu, J., Ma, Z., Fan, C. W., Wei, S., Hao, W., Kilgore, J., Williams, N. S. et al. (2009a). Small molecule-mediated disruption of Wnt-dependent signaling in tissue regeneration and cancer. *Nat. Chem. Biol.* **5**, 100-107.

Chen, J., Watanabe, M., Huang, P., Sakaguchi, M., Ochiai, K., Nasu, Y., Ouchida, M., Huh, N. H., Shimizu, K., Kashiwakura, Y. et al. (2009b). REIC/Dkk-3 stable transfection reduces the malignant phenotype of mouse prostate cancer RM9 cells. *Int. J. Mol. Med.* **24**, 789-794.

Clevers, H. (2006). Wnt/beta-catenin signaling in development and disease. *Cell* **127**, 469-480.

Debnath, J., Mills, K. R., Collins, N. L., Reginato, M. J., Muthuswamy, S. K. and Brugge, J. S. (2002). The role of apoptosis in creating and maintaining luminal space within normal and oncogene-expressing mammary acini. *Cell* **111**, 29-40.

Debnath, J., Muthuswamy, S. K. and Brugge, J. S. (2003). Morphogenesis and oncogenesis of MCF-10A mammary epithelial acini grown in three-dimensional basement membrane cultures. *Methods* **30**, 256-268.

del Barco Barrantes, I., Montero-Pedrazuela, A., Guadaño-Ferraz, A., Obregon, M. J., Martinez de Mena, R., Gailus-Durner, V., Fuchs, H., Franz, T. J., Kalaydjiev, S., Klempt, M. et al. (2006). Generation and characterization of dickkopf3 mutant mice. *Mol. Cell. Biol.* **26**, 2317-2326.

Dennler, S., Itoh, S., Vivien, D., ten Dijke, P., Huet, S. and Gauthier, J. M. (1998). Direct binding of Smad3 and Smad4 to critical TGF beta-inducible elements in the promoter of human plasminogen activator inhibitor-type 1 gene. *EMBO J.* **17**, 3091-3100.

Edamura, K., Nasu, Y., Takaishi, M., Kobayashi, T., Abarzua, F., Sakaguchi, M., Kashiwakura, Y., Ebara, S., Saika, T., Watanabe, M. et al. (2007). Adenovirus-mediated REIC/Dkk-3 gene transfer inhibits tumor growth and metastasis in an orthotopic prostate cancer model. *Cancer Gene Ther.* **14**, 765-772.

Francis, J. C., McCarthy, A., Thomsen, M. K., Ashworth, A. and Swain, A. (2010). Brca2 and Trp53 deficiency cooperate in the progression of mouse prostate tumourigenesis. *PLoS Genet.* **6**, e1000995.

Giannini, A. L., Vivanco, M. and Kypta, R. M. (2000). alpha-catenin inhibits beta-catenin signaling by preventing formation of a beta-catenin*T-cell factor*DNA complex. *J. Biol. Chem.* **275**, 21883-21888.

Glinka, A., Wu, W., Delius, H., Monaghan, A. P., Blumenstock, C. and Niehrs, C. (1998). Dickkopf-1 is a member of a new family of secreted proteins and functions in head induction. *Nature* **391**, 357-362.

Gu, Y. M., Ma, Y. H., Zhao, W. G. and Chen, J. (2011). Dickkopf3 overexpression inhibits pancreatic cancer cell growth in vitro. *World J. Gastroenterol.* **17**, 3810-3817.

Guo, H. B., Johnson, H., Randolph, M., Nagy, T., Blalock, R. and Pierce, M. (2010). Specific posttranslational modification regulates early events in mammary carcinoma formation. *Proc. Natl. Acad. Sci. USA* **107**, 21116-21121.

Härmä, V., Virtanen, J., Mäkelä, R., Happonen, A., Mpindi, J. P., Knuuttila, M., Kohonen, P., Lötjönen, J., Kallioniemi, O. and Nees, M. (2010). A comprehensive panel of three-dimensional models for studies of prostate cancer growth, invasion and drug responses. *PLoS ONE* **5**, e10431.

Hoang, B. H., Kubo, T., Healey, J. H., Yang, R., Nathan, S. S., Kolb, E. A., Mazza, B., Meyers, P. A. and Gorlick, R. (2004). Dickkopf 3 inhibits invasion and motility of Saos-2 osteosarcoma cells by modulating the Wnt-beta-catenin pathway. *Cancer Res.* **64**, 2734-2739.

Hsu, R. J., Lin, C. C., Su, Y. F. and Tsai, H. J. (2011). dickkopf-3-related gene regulates the expression of zebrafish myf5 gene through phosphorylated p38a-dependent Smad4 activity. *J. Biol. Chem.* **286**, 6855-6864.

Inman, G. J. (2011). Switching TGFβ from a tumor suppressor to a tumor promoter. *Curr. Opin. Genet. Dev.* **21**, 93-99.

Jinnin, M., Ihn, H. and Tamaki, K. (2006). Characterization of SIS3, a novel specific inhibitor of Smad3, and its effect on transforming growth factor-beta1-induced extracellular matrix expression. *Mol. Pharmacol.* **69**, 597-607.

Jones, E., Pu, H. and Kyprianou, N. (2009). Targeting TGF-beta in prostate cancer: therapeutic possibilities during tumor progression. *Expert Opin. Ther. Targets* **13**, 227-234.

Kane, N., Jones, M., Brosens, J. J., Saunders, P. T., Kelly, R. W. and Critchley, H. O. (2008). Transforming growth factor-beta1 attenuates expression of both the progesterone receptor and Dickkopf in differentiated human endometrial stromal cells. *Mol. Endocrinol.* **22**, 716-728.

Kashiwakura, Y., Ochiai, K., Watanabe, M., Abarzua, F., Sakaguchi, M., Takaoka, M., Tanimoto, R., Nasu, Y., Huh, N. H. and Kumon, H. (2008). Down-regulation of inhibition of differentiation-1 via activation of activating transcription factor 3 and Smad regulates REIC/Dickkopf-3-induced apoptosis. *Cancer Res.* **68**, 8333-8341.

Kawano, Y., Kitaoka, M., Hamada, Y., Walker, M. M., Waxman, J. and Kypta, R. M. (2006). Regulation of prostate cell growth and morphogenesis by Dickkopf-3. *Oncogene* **25**, 6528-6537.

Kawano, Y., Diez, S., Uysal-Onganer, P., Darrington, R. S., Waxman, J. and Kypta, R. M. (2009). Secreted Frizzled-related protein-1 is a negative regulator of androgen receptor activity in prostate cancer. *Br. J. Cancer* **100**, 1165-1174.

Krupnik, V. E., Sharp, J. D., Jiang, C., Robison, K., Chickering, T. W., Amaravadi, L., Brown, D. E., Guyot, G., Mays, G., Leiby, K. et al. (1999). Functional and structural diversity of the human Dickkopf gene family. *Gene* **238**, 301-313.

Kypta, R. M. and Waxman, J. (2012). Wnt/beta-catenin signaling in prostate cancer. *Nat. Rev. Urol.* **9**, 418-428.

Lee, G. Y., Kenny, P. A., Lee, E. H. and Bissell, M. J. (2007). Three-dimensional culture models of normal and malignant breast epithelial cells. *Nat. Methods* **4**, 359-365.

Lee, E. J., Jo, M., Rho, S. B., Park, K., Yoo, Y. N., Park, J., Chae, M., Zhang, W. and Lee, J. H. (2009). Dkk3, downregulated in cervical cancer, functions as a negative regulator of beta-catenin. *Int. J. Cancer* **124**, 287-297.

Liu, R., Zhou, Z., Huang, J. and Chen, C. (2011). PMEPA1 promotes androgen receptor-negative prostate cell proliferation through suppressing the Smad3/4-c-Myc-p21 Cip1 signaling pathway. *J. Pathol.* **223**, 683-694.

Lodygin, D., Epanchintsev, A., Menssen, A., Diebold, J. and Hermeking, H. (2005). Functional epigenomics identifies genes frequently silenced in prostate cancer. *Cancer Res.* **65**, 4218-4227.

Mao, B. and Niehrs, C. (2003). Kremen2 modulates Dickkopf2 activity during Wnt/LRP6 signaling. *Gene* **302**, 179-183.

Mao, B., Wu, W., Li, Y., Hoppe, D., Stannek, P., Glinka, A. and Niehrs, C. (2001). LDL-receptor-related protein 6 is a receptor for Dickkopf proteins. *Nature* **411**, 321-325.

Massagué, J. (2008). TGFbeta in Cancer. *Cell* **134**, 215-230.

Matsuyama, S., Iwadate, M., Kondo, M., Saitoh, M., Hanyu, A., Shimizu, K., Aburatani, H., Mishima, H. K., Imamura, T., Miyazono, K. et al. (2003). SB-431542 and Gleevec inhibit transforming growth factor-beta-induced proliferation of human osteosarcoma cells. *Cancer Res.* **63**, 7791-7798.

Mazor, M., Kawano, Y., Zhu, H., Waxman, J. and Kypta, R. M. (2004). Inhibition of glycogen synthase kinase-3 represses androgen receptor activity and prostate cancer cell growth. *Oncogene* **23**, 7882-7892.

Nakamura, R. E. and Hackam, A. S. (2010). Analysis of Dickkopf3 interactions with Wnt signaling receptors. *Growth Factors* **28**, 232-242.

Niehrs, C. (2006). Function and biological roles of the Dickkopf family of Wnt modulators. *Oncogene* **25**, 7469-7481.

Ochiai, K., Watanabe, M., Ueki, H., Huang, P., Fujii, Y., Nasu, Y., Noguchi, H., Hirata, T., Sakaguchi, M., Huh, N. H. et al. (2011). Tumor suppressor REIC/Dkk-3 interacts with the dynein light chain, Tctex-1. *Biochem. Biophys. Res. Commun.* **412**, 391-395.

Onai, T., Takai, A., Setiamarga, D. H. and Holland, L. Z. (2012). Essential role of Dkk3 for head formation by inhibiting Wnt/β-catenin and Nodal/Vg1 signaling pathways in the basal chordate amphioxus. *Evol. Dev.* **14**, 338-350.

Papatriantafyllou, M., Moldenhauer, G., Ludwig, J., Tafuri, A., Garbi, N., Hollmann, G., Küblbeck, G., Klevenz, A., Schmitt, S., Pougialis, G. et al. (2012). Dickkopf-3, an immune modulator in peripheral CD8 T-cell tolerance. *Proc. Natl. Acad. Sci. USA* **109**, 1631-1636.

Pinho, S. and Niehrs, C. (2007). Dkk3 is required for TGF-beta signaling during Xenopus mesoderm induction. *Differentiation* **75**, 957-967.

Salm, S. N., Burger, P. E., Coetzee, S., Goto, K., Moscatelli, D. and Wilson, E. L. (2005). TGF-beta maintains dormancy of prostatic stem cells in the proximal region of ducts. *J. Cell Biol.* **170**, 81-90.

Shappell, S. B., Thomas, G. V., Roberts, R. L., Herbert, R., Ittmann, M. M., Rubin, M. A., Humphrey, P. A., Sundberg, J. P., Rozengurt, N., Barrios, R. et al. (2004). Prostate pathology of genetically engineered mice: definitions and classification. The consensus report from the Bar Harbor meeting of the Mouse Models of Human Cancer Consortium Prostate Pathology Committee. *Cancer Res.* **64**, 2270-2305.

Singha, P. K., Yeh, I. T., Venkatachalam, M. A. and Saikumar, P. (2010). Transforming growth factor-beta (TGF-beta)-inducible gene TMEPAI converts TGF-beta from a tumor suppressor to a tumor promoter in breast cancer. *Cancer Res.* **70**, 6377-6383.

Sugimura, Y., Cunha, G. R. and Donjacour, A. A. (1986). Morphogenesis of ductal networks in the mouse prostate. *Biol. Reprod.* **34**, 961-971.

Tobin, S. W., Douville, K., Benbow, U., Brinckerhoff, C. E., Memoli, V. A. and Arrick, B. A. (2002). Consequences of altered TGF-beta expression and responsiveness in breast cancer: evidence for autocrine and paracrine effects. *Oncogene* **21**, 108-118.

Tokar, E. J., Ancrile, B. B., Cunha, G. R. and Webber, M. M. (2005). Stem/progenitor and intermediate cell types and the origin of human prostate cancer. *Differentiation* **73**, 463-473.

Tsuji, T., Miyazaki, M., Sakaguchi, M., Inoue, Y. and Namba, M. (2000). A REIC gene shows down-regulation in human immortalized cells and human tumor-derived cell lines. *Biochem. Biophys. Res. Commun.* **268**, 20-24.

Tudzarova, S., Trotter, M. W., Wollenschlaeger, A., Mulvey, C., Godovac-Zimmermann, J., Williams, G. H. and Stoeber, K. (2010). Molecular architecture of the DNA replication origin activation checkpoint. *EMBO J.* **29**, 3381-3394.

Tyson, D. R., Inokuchi, J., Tsunoda, T., Lau, A. and Ornstein, D. K. (2007). Culture requirements of prostatic epithelial cell lines for acinar morphogenesis and lumen formation in vitro: role of extracellular calcium. *Prostate* **67**, 1601-1613.

Ueno, K., Hirata, H., Majid, S., Chen, Y., Zaman, M. S., Tabatabai, Z. L., Hinoda, Y. and Dahiya, R. (2011). Wnt antagonist DICKKOPF-3 (Dkk-3) induces apoptosis in human renal cell carcinoma. *Mol. Carcinog.* **50**, 449-457.

Uysal-Onganer, P., Kawano, Y., Caro, M., Walker, M. M., Diez, S., Darrington, R. S., Waxman, J. and Kypta, R. M. (2010). Wnt-11 promotes neuroendocrine-like differentiation, survival and migration of prostate cancer cells. *Mol. Cancer* **9**, 55.

Veeck, J. and Dahl, E. (2012). Targeting the Wnt pathway in cancer: the emerging role of Dickkopf-3. *Biochim. Biophys. Acta* **1825**, 18-28.

Veeman, M. T., Slusarski, D. C., Kaykas, A., Louie, S. H. and Moon, R. T. (2003). Zebrafish prickle, a modulator of noncanonical Wnt/Fz signaling, regulates gastrulation movements. *Curr. Biol.* **13**, 680-685.

Webber, M. M., Bello, D., Kleinman, H. K. and Hoffman, M. P. (1997). Acinar differentiation by non-malignant immortalized human prostatic epithelial cells and its loss by malignant cells. *Carcinogenesis* **18**, 1225-1231.

Webber, M. M., Quader, S. T., Kleinman, H. K., Bello-DeOcampo, D., Storto, P. D., Bice, G., DeMendonca-Calaca, W. and Williams, D. E. (2001). Human cell lines as an in vitro/in vivo model for prostate carcinogenesis and progression. *Prostate* **47**, 1-13.

Yue, W., Sun, Q., Dacic, S., Landreneau, R. J., Siegfried, J. M., Yu, J. and Zhang, L. (2008). Downregulation of Dkk3 activates beta-catenin/TCF-4 signaling in lung cancer. *Carcinogenesis* **29**, 84-92.

Zenzmaier, C., Untergasser, G., Hermann, M., Dirnhofer, S., Sampson, N. and Berger, P. (2008). Dysregulation of Dkk-3 expression in benign and malignant prostatic tissue. *Prostate* **68**, 540-547.

Zhang, Q., Helfand, B. T., Jang, T. L., Zhu, L. J., Chen, L., Yang, X. J., Kozlowski, J., Smith, N., Kundu, S. D., Yang, G. et al. (2009). Nuclear factor-kappaB-mediated transforming growth factor-beta-induced expression of vimentin is an independent predictor of biochemical recurrence after radical prostatectomy. *Clin. Cancer Res.* **15**, 3557-3567.
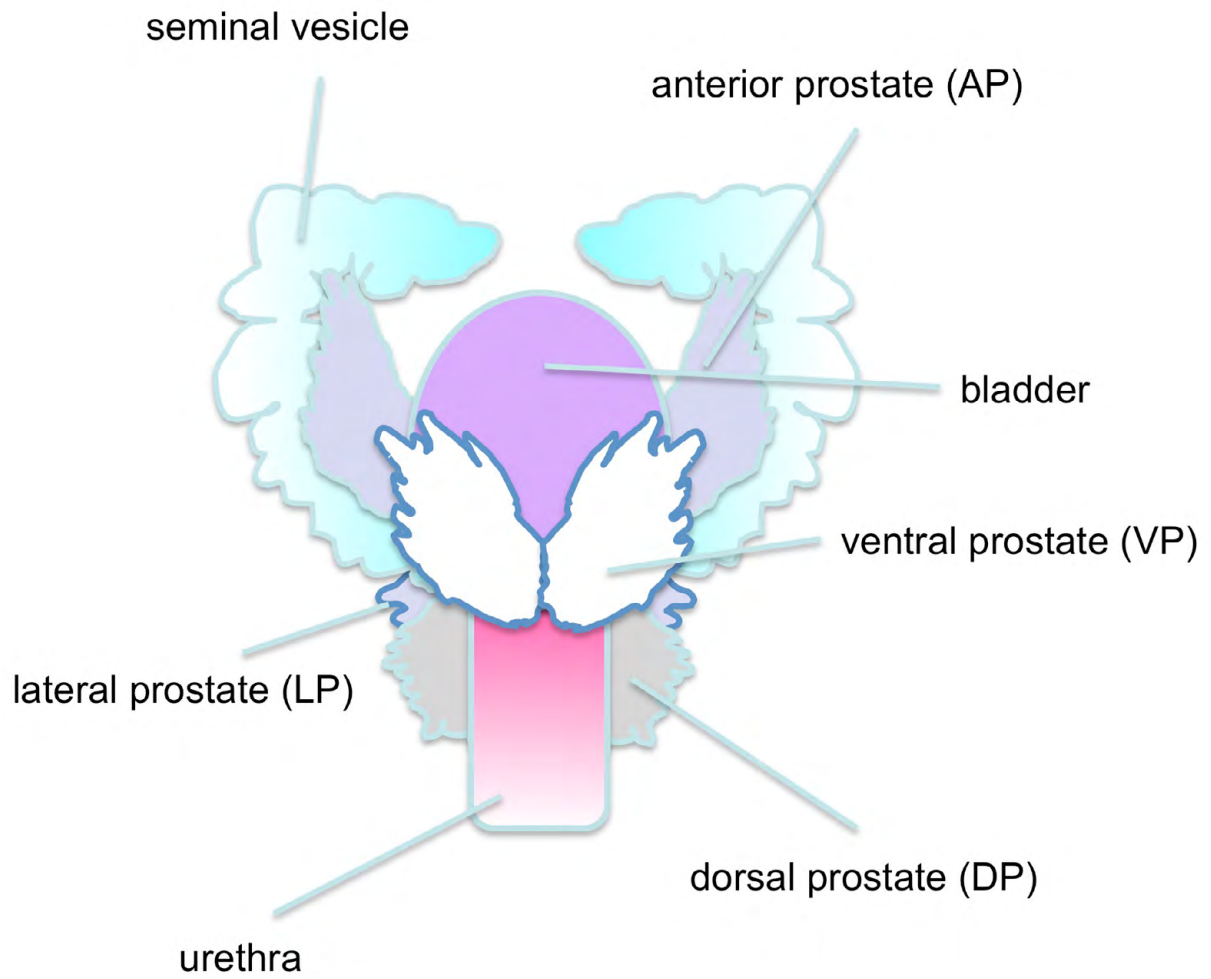
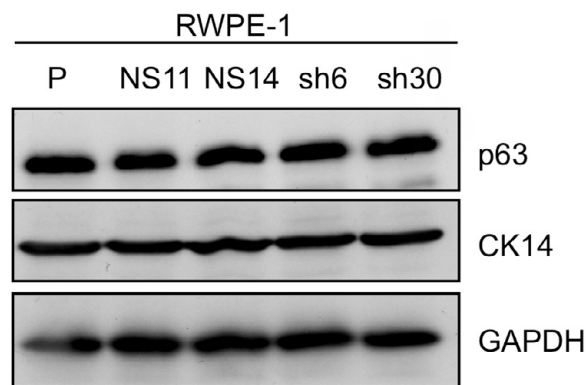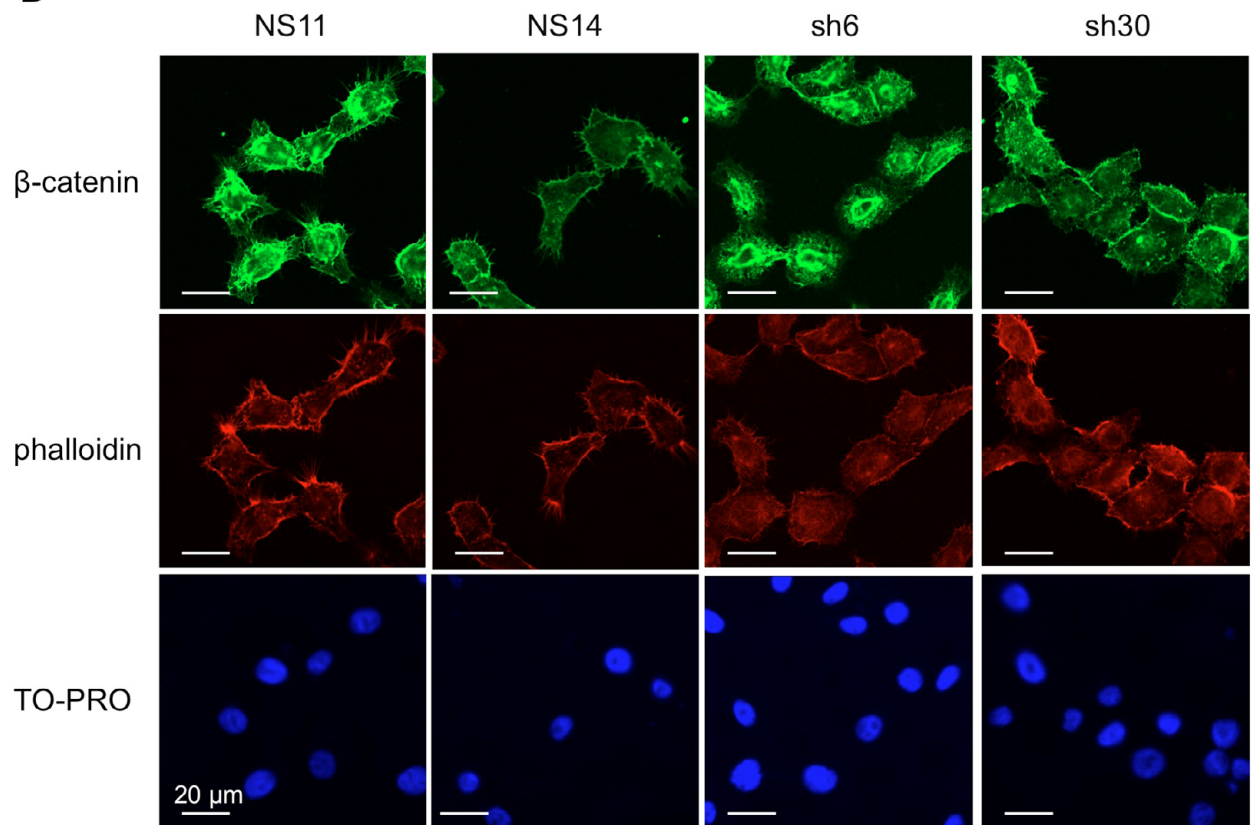**Fig. S1.** Cartoon depicting the male urogenital system in adult mice indicating the prostatic lobes.

Fig. S2. Phenotypic and morphological characterization of Dkk-3-silenced RWPE-1 sublines. (A) Western blot for p63 and CK14 in RWPE-1 parental cells (P), Dkk-3 depleted clones (sh6 and sh30), and non-silenced control clones (NS11 and NS14). GAPDH was used as a loading control. (B) Immunostaining for β-catenin (green) and F-actin (red, detected using fluorescent phalloidin) in the indicated RWPE-1 sublines; nuclei were stained using TO-PRO-3 (blue).
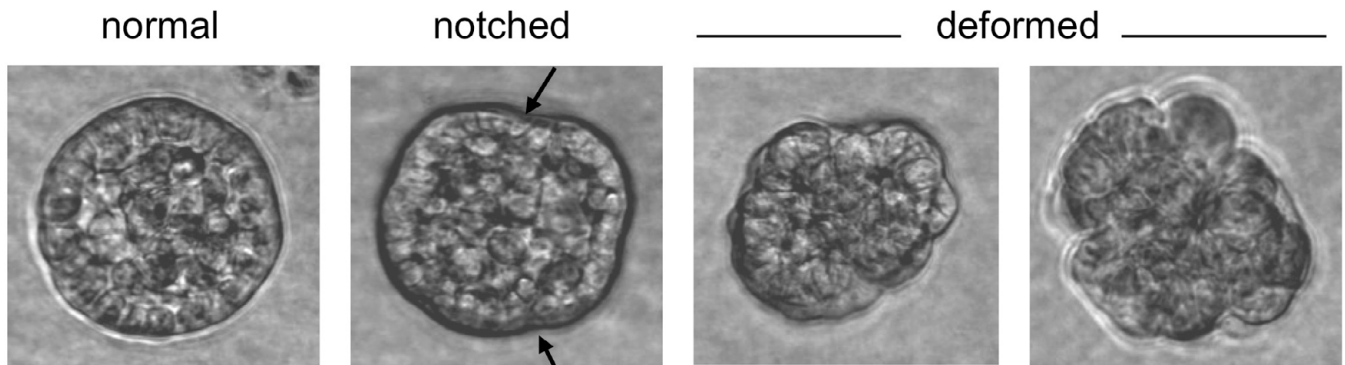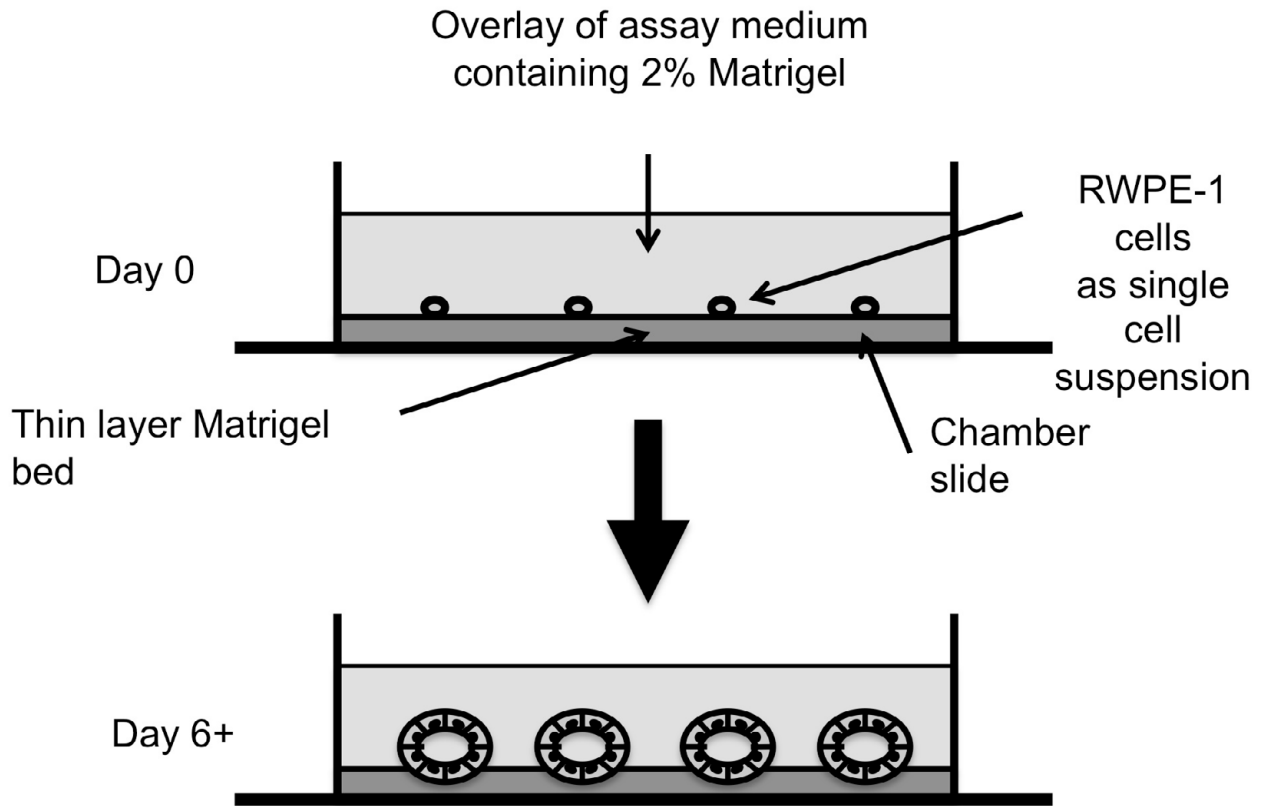
Fig. S3. RWPE-1 acinar morphogenesis assays. Top: schematic diagram of the acinar morphogenesis assay of RWPE-1 cells on Matrigel (adapted from Debnath (Debnath et al., 2003)). RWPE-1 cells are seeded as a single-cell suspension in assay medium containing 2% FCS, 5 ng/ml EGF and 2% Matrigel onto a thin layer bed of solidified Matrigel. The assay medium is replaced every the other day and acinar formation usually becomes apparent by day 6. Bottom: Acinar morphogenesis phenotypes observed in RWPE-1 derived sublines. Representative examples of 'normal', 'notched' (acini with irregular periphery) and 'deformed' (amorphous aggregation without trace of acinar structure) are shown.
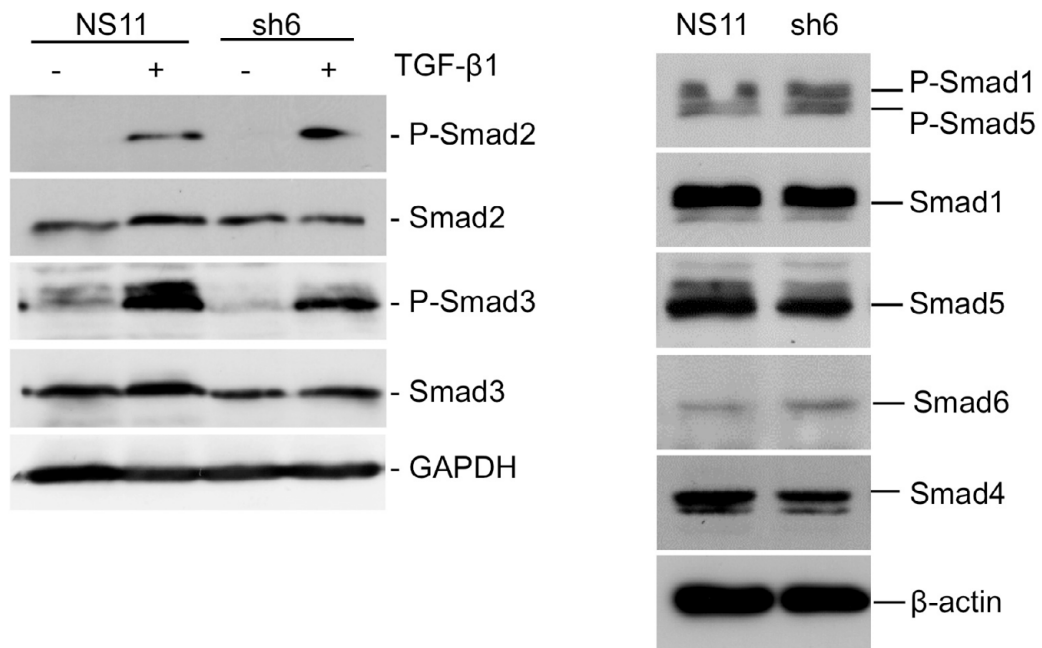
Fig. S4. Expression and phosphorylation of Smad proteins in Dkk-3-silenced cells. Extracts from the RWPE-1 NS11 and sh6 cells (left panels treated for 1 h with vehicle (PBS) or 1 ng/ml TGF-β1) were probed by western blotting for the indicated proteins.
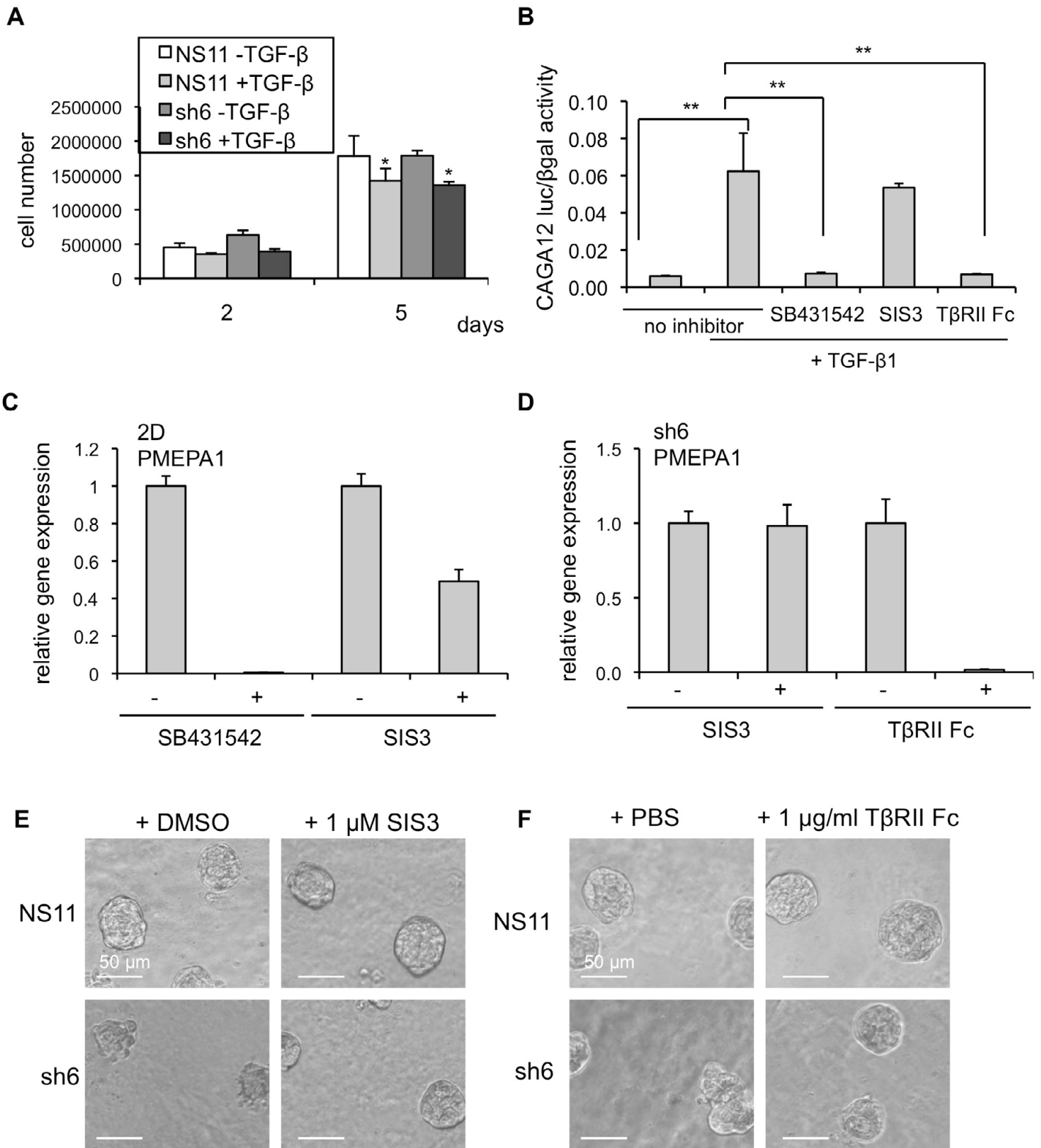
Fig. S5. Effects of TGF-β and TGF-β signalling inhibitors on RWPE-1 cells. (**A**) Cell proliferation assays for RWPE-1 sublines cultured as monolayers. 2.5×10^5 cells were plated in triplicate for each time point and cells were counted after 2 and 5 days. The average and s.d. of cell number are shown from a representative experiment (n=3). TGF-β treatment reduces cell number in sh6 and NS11 cells at 5 days; *P<0.05 Student's t test, P=0.12 (NS11) and 0.12 (sh6) at 2 days. (**B**) Effects of TGF-β signalling inhibitors on CAGA-luciferase activity. RWPE-1 sh6 cells transfected with pGL3-CAGA12-luciferase and pDM-β-gal, untreated or treated with TGF-β1 (1 ng/ml) and either SB431542 (1 μM), SIS3 (1 μM), TGFβRII-Fc (1 μg/ml) or an equivalent volume of vehicle (DMSO or PBS, in the case of TGFβRII-Fc) for 21 h were assayed for gene reporter activity; **P<0.001 vs TGF-β1, Student's t test, n=3. (**C**) Effects of TGF-β signalling inhibitors on PMEPA1 expression. Graph shows relative expression of PMEPA1 in RWPE-1 NS11 cells growing as a monolayer (2D), as determined by q-PCR. (**D**) Effects of TGF-β signalling inhibitors on PMEPA1 expression. Graph shows relative expression of PMEPA1 in RWPE-1 sh6 cells growing in 3D, as determined by q-PCR. (**E**) Representative images of acini from the experiment shown in Fig. 6D. (**F**) Representative images of acini from the experiment shown in Fig. 6E.